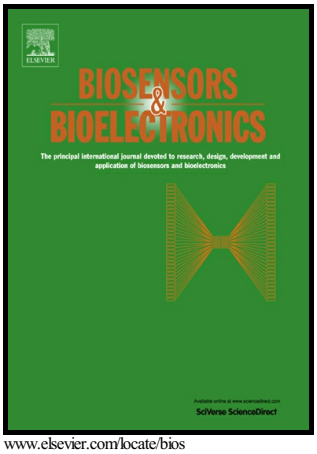

www.elsevier.com/locate/bios

Novel Amine-Functionalized Iron Trimesates with Enhanced Peroxidase-Like Activity and their Applications for the Fluorescent Assay of Choline and Acetylcholine

Anil H. Valekar, Bhagwan S. Batule, Moon Il Kim, Kyung-Ho Cho, Do-Young Hong, U-Hwang Lee, Jong-San Chang, Hyun Gyu Park, Young Kyu Hwang

PII: S0956-5663(17)30592-4
DOI: http://dx.doi.org/10.1016/j.bios.2017.08.056
Reference: BIOS9966

To appear in: *Biosensors and Bioelectronic*

Received date: 29 April 2017
Revised date: 21 August 2017
Accepted date: 25 August 2017

Cite this article as: Anil H. Valekar, Bhagwan S. Batule, Moon Il Kim, Kyung-Ho Cho, Do-Young Hong, U-Hwang Lee, Jong-San Chang, Hyun Gyu Park and Young Kyu Hwang, Novel Amine-Functionalized Iron Trimesates with Enhanced Peroxidase-Like Activity and their Applications for the Fluorescent Assay of Choline and Acetylcholine, *Biosensors and Bioelectronic,* http://dx.doi.org/10.1016/j.bios.2017.08.056

Novel Amine-Functionalized Iron Trimesates with Enhanced Peroxidase-Like Activity and their Applications for the Fluorescent Assay of Choline and Acetylcholine

Anil H. Valekar, [# a,b] Bhagwan S. Batule, [# c] Moon Il Kim, [d] Kyung-Ho Cho, [a] Do-Young Hong, [a,b] U-Hwang Lee, [a,b] Jong-San Chang[a,e] , Hyun Gyu Park *[c] and Young Kyu Hwang*[a,b]

[a] Research Group of Nanocatalysts, Korea Research Institute of Chemical Technology (KRICT), Daejeon 34114, Korea

[b] Department of Advanced Materials and Chemical Engineering, University of Science and Technology (UST), 217 Gajeong-Ro, Yuseong, Daejeon 34113, Korea

[c] Chemical & Biomolecular Engineering (BK21+ Program), KAIST, 291 Deahak-ro, Yuseong-gu, Daejeon 34141, Korea

[d] Department of BioNano Technology, Gachon University, 1342 Seongnamdae-ro, Sujeong-gu, Seongnam, Gyeonggi 13120, Korea

[e] Department of Chemistry, Sungkyunkwan University, Suwon 16419, Korea

E-mail: hgpark@kaist.ac.kr and ykhwang@krict.re.kr

[#] These authors contributed equally to this work.

Abstract

We herein describe novel amine-grafted metal–organic frameworks (MOFs) as a promising alternative to natural peroxidase enzyme and their applications for a fluorescent assay of choline (Cho) and acetylcholine (ACh). Among diverse amine-functionalized MOFs, *N*,*N*,*N*′,*N*′-tetramethyl-1,4-butanediamine (TMBDA)-functionalized MIL-100(Fe) (TMBDA-MIL-100(Fe)) exhibited the highest peroxidase activity by developing intense fluorescence from Amplex UltraRed (AUR) in the presence of H_2O_2, which was presumably due to the synergetic effect of the enhanced negative potential and precisely controlled molecular size of the grafted diamine. Based on the excellent peroxidase-like activity of TMBDA-MIL-100(Fe), choline and ACh were reliably determined down to 0.027 and 0.036 μM, respectively. Furthermore, practical applicability of this strategy was successfully demonstrated by detecting choline and ACh in spiked samples of milk and serum, respectively. This work highlights the advantages of amine-grafted MOFs for the preparation of biomimetic catalysts, extending their scope to biosensor applications.

Keywords: Metal–organic framework, amine grafting, peroxidase-like activity, choline detection, acetylcholine detection

1. Introduction

Natural horseradish peroxidase (HRP) is an important heme-containing enzyme that has been studied for more than a century (Filizola and Loew 2000). In biological processes, peroxidases act as catalysts and are capable of promoting the oxidation of a substrate by the decomposition of oxides or peroxides with high efficiency, such as H_2O_2 (Rodríguez-López et al. 2001). HRP continues to attract considerable attention from researchers across a variety of disciplines because of its widespread practical and commercial applications (Veitch 2004). However, HRP is a protein that also suffers from several serious disadvantages, such as instability and easy loss of catalytic activity in harsh environments as well as high cost and time-consuming preparation and purification procedures (Feng et al. 2012; Rodríguez-López et al. 2001). Thus, the synthesis and development of mimics of HRP to improve its catalytic performance are of great significance (Wei and Wang 2013) and many researchers have made huge efforts to develop the enzyme mimics in recent years. Since the first peroxidase mimics based on Fe_3O_4 nanoparticles which was reported by Gao *et al*., (Gao et al. 2007) a variety of nanomaterials, such as Pt nanoparticles (NPs) (He et al. 2014), Co_3O_4 NPs (Mu et al. 2012), carbon nanodots (Shi et al. 2011), CeO_2 NPs (Asati et al. 2009), graphene oxides (Song et al. 2010b), single-walled carbon nanotubes (Song et al. 2010c), and their composites (Kim et al. 2011a; Kim et al. 2014a; Kim et al. 2014b), have been demonstrated to show peroxidase-mimicking activity. These peroxidase mimics are generally more stable than HRP and have tunable catalytic activities. Nevertheless, they usually exhibit a relatively low catalytic

activity compared with HRP and laborious procedures are often required for their preparation and further surface functionalization (Qin et al. 2013). Therefore, the development of a new generation of peroxidase-mimicking nanomaterials obtainable by simple preparation procedures, with high catalytic activity as well as excellent stability, is still a hot topic.

Recently, biosensors based on enzyme-mimicking organic-inorganic hybrid nanomaterials such as protein or DNA-Cu nanoflowers (Batule et al. 2015; Park et al. 2017), Fe-aminoclay (Lee et al. 2013), and MOFs (Ai et al. 2013; Dong et al. 2015; Feng et al. 2012; Liu et al. 2013; Qin et al. 2013; Zhang et al. 2014) have been successfully exploited. Among these, MOFs have emerged as a new class of crystalline hybrid porous materials by taking advantages of their intriguing structural properties such as high specific surface area, tunable pore size distribution, coordinatively unsaturated metal sites (CUS) in the skeleton, and practically limitless choice of metals and organic ligands affording an essentially infinite number of possible combinations. These fascinating features led them to be widely used in many fields, such as gas storage (Llewellyn et al. 2008; Murray et al. 2009), gas separation (Li et al. 2012; Wuttke et al. 2012), catalysis (Horcajada et al. 2007; Lee et al. 2009; Valekar et al. 2016), and sensing (Desai et al. 2015; Kumar et al. 2015; Meilikhov et al. 2013; Nagarkar et al. 2013). Besides their aforementioned unique properties, MOFs provide great potential for the further functionalization of their structures. According to the literature, post synthetic modification (PSM, where one can do the modification in original MOF structure after its synthesis) is considered as the most common method to achieve the desired

functionality in MOFs, subsequently, anticipated chemical and physical property can be imparted (Tanabe and Cohen 2011). Therefore, a large number of functional MOFs have been prepared using the PSM and successfully utilized to improve their performance in catalysis (Banerjee et al. 2009; Hwang et al. 2008; Kasinathan et al. 2011) and gas storage (Dinca et al. 2007; Wang and Cohen 2009). However, functionalized MOFs containing redox-active metal centers have rarely been used as peroxidase mimics mainly due to their hydrothermal and chemical instability (Larsen et al. 2011; Qin et al. 2013).

The previous reported MOF biosensors are simply used either as synthesized Fe based MOFs such as MIL-53, MIL-68, MIL-88-NH_2, MIL-100, and MIL-101, or Hemin@MIL-101(Al)-NH_2 composite for peroxidase mimics (Ai et al. 2013; Dong et al. 2015; Feng et al. 2012; Liu et al. 2013; Qin et al. 2013; Zhang et al. 2014). However, these studies did not utilize one of the most promising approaches of functionalizing MOF on CUS with desired functionality. In this work, we took this opportunity for the first time and functionalized MIL-100(Fe) by grafting various aliphatic diamines on its CUS. The performance of functionalized MIL-100(Fe) for peroxidase mimic activity enhanced significantly compared to its pristine form presumably due to the synergetic effect of the enhanced negative potential and precisely controlled molecular size of the grafted diamines. Based on this enhanced peroxidase-like activity, we developed a simple and effective fluorescent method for the quantitative determination of choline and acetylcholine. These two biomolecules serve as important regulators in many biological processes including nutrition and neurotransmission,

however until now, their detection methods have been suffered from many limitations such as low sensitivity, unstable signal, and complex experimental steps (Chen et al. 2011). Thus, there is a significant incentive to develop sensitive, reliable, and convenient assay of choline and acetylcholine. Herein, we used amine-functionalized MOFs coupled with enzymes specific for choline and acetylcholine for the successful detection of choline and acetylcholine even present in spiked samples of milk and serum, respectively.

2. Experimental Section

2.1. Synthesis, amine grafting on CUS of MIL-100(Fe) and its characterizations

Fluorine-free biocompatible MIL-100(Fe) was synthesized using a scaled up method previously reported by our group (Seo et al. 2012). Amine grafting on CUS of MIL-100(Fe) and their characterizations has been described in details in experimental part of the supporting information.

2.3.Peroxidase-like activity of MOFs with AUR and TMB substrates

The peroxidase-like activity of the different MOFs was measured in a 50 µL reaction solution containing H_2O_2 (1 mM), MOF (0.2 mg/mL), and 3,3′,5,5′-tetramethylbenzidine (TMB) (1 mM) or AUR (50 µM) as colorimetric or fluorogenic substrate, respectively, in Tris acetate buffer (5 mM, pH 7) on the basis of the absorbance recorded at 500-700 nm (maximum at 650 nm) and fluorescence at Ex-540 nm and Em-570-650 nm (maximum at 588 nm). The

fluorescence intensities were measured using a Tecan Infinite M200 pro microplate reader (Mannedorf, Switzerland) with black, 384-well Greinier Bio-one microplates (ref: 781077, Courtaboeuf, France).

2.4. Quantification of choline and acetylcholine

Detailed description on quantification of choline and acetylcholine can be found in supporting information of the manuscript.

3. Results and discussion

3.1. Amine grafting on CUS of MIL-100(Fe)

The present biosensor system for fluorescent quantification of Cho and ACh consists of acetylcholine esterase (AChE) and choline oxidase (ChOx), which would generate H_2O_2 by their consecutive catalytic oxidation from acetylcholine. This would activate amine-functionalized MOF to convert selected substrate, AUR, into highly fluorogenic product (oxAUR) (**Figure 1a**). For the development of functional MOFs with enhanced peroxidase-like activity, the post-synthetic amine functionalization was carried out by grafting of diamines on the CUS of MIL-100(Fe), as illustrated in **Figure 1b**. The diamine compounds used for the functionalization include ethylene diamine (ED), *N,N′*-dimethyl-1,3-propanediamine (DMPDA), and *N,N,N′,N′*-tetramethyl-1,4-butanediamine (TMBDA).

The stability of the amine modified MIL-100(Fe) frameworks was investigated using X-ray powder diffraction analysis (XRPD) (**Figure 2a**). The powder diffraction patterns of the functionalized samples showed decreased peak intensity compared to the pristine MOF. This result is consistent with previous reports showing a reduction in the peak intensity due to the incorporation of diamines in the pores of MOFs (Hwang et al. 2008; Kasinathan et al. 2011). The textural properties of the pristine and amine-functionalized samples are given in **Table S1**. After amine functionalization, both surface area and pore volume decreased due to different diamines that were attached to the pore surfaces and partially blocked the pores. However, the N_2 adsorption isotherm patterns remained intact after functionalization (**Figure 2b**). The pore size distribution (PSD) profiles calculated on the basis of the density functional theory (DFT) showed no significant change in the pore size of MIL-100(Fe) after amine grafting (**Figure S1**), probably due to the low amine loading determined from the "N" content (Table S1). The grafting of diamines onto the CUS of MIL-100(Fe) occurred to a reasonably lower extent when compared with the diamine grafting on the CUS of MIL-101(Cr) and MIL-100(Cr), which was previously reported by Hwang *et al*. (Hwang et al. 2008; Kasinathan et al. 2011) and Cabello *et al*. (Cabello et al. 2015), respectively. This indicates that a change of the metal center in the framework of MIL-100 (Fe instead of Cr) can affect the chelating reaction of the amines with the metal in MOFs. This assumption could be further supported by the electronic configuration of the Fe(III) center present in MIL-100(Fe). The octahedral unit of Fe(III) possesses a high spin state resulting in a large

exchange energy of electrons in the subshell (Horcajada et al. 2007). Nevertheless, it has been proved that the anchoring of a small amount (0.02 mmol/g) of "N" containing polymer on the surface of MIL-100(Fe) can considerably affect its magnetic resonance imaging activity for use in theranostic applications (Zimpel et al. 2016). Thus, these results encouraged us to continue our work in view of potential biosensing applications.

The amine grafting was further confirmed by Fourier transform infrared (FT-IR) spectroscopy. **Figure 2c** shows the spectrum of bare MIL-100(Fe) compared with those of different amine-grafted MIL-100(Fe) compounds**.** Despite the presence of amine moieties in the framework, no major changes in the FT-IR patterns were observed due to the low levels of amine grafting. However, two amine-grafted samples, ED-MIL-100(Fe) and DMPDA-MIL-100(Fe), showed a small additional absorption band in the region of 3250-3350 cm^{-1}, which could be attributed to the characteristic N-H stretching vibration mode, as marked in Figure 2c. The lack of N-H bonds in TMBDA-MIL-100(Fe) produced no additional peak in this region. The parent MIL-100(Fe) showed an absorption peak at 1739 cm^{-1} corresponding to the C=O stretching and indicating the presence of free trimesic acid, which decreased in intensity and slightly shifted to the lower wavelength of 1733 cm^{-1} after modification with primary (ED) and secondary (DMPDA) amines. This suggests that these amine groups can probably form hydrogen bonds with the free trimesic acid. TMBDA-MIL-100(Fe) did not show any change in the C=O stretching frequency, which might be due to the absence of N-H bonds in TMBDA available for hydrogen bonding. In order to show the presence of the

amines on the surface of MIL-100(Fe), we performed X-ray photoelectron spectroscopy (XPS) analysis (**Figure 2d**). The N 1s peak around 397 eV due to the amine groups was observed in all amine-grafted samples and revealed the occurrence of amine moieties on the surface of the amine-grafted MIL-100(Fe) samples. The presence of surface amine functionalities affected the surface charge of the MIL-100(Fe) particles, which was evident from the zeta potential measured at neutral pH in an aqueous medium (Table S1). It can be seen that the negative potentials of all three amine modified MOFs increased compared to their unmodified counterpart. These results clearly show that the surface charge of the amine-grafted MIL-100(Fe) particles is dependent on the nature of the amine, and could further give rise to different peroxidase mimetic activities.

3.2. Peroxidase-like activity of amine-grafted MIL-100(Fe)

To develop a new strategy for sensing of biomolecules, different amine-grafted MOFs such as ED-MIL-100(Fe), DMPDA-MIL-100(Fe), and TMBDA-MIL-100(Fe) along with the pristine MIL-100(Fe) were examined for their peroxidase-like activities to promote the oxidation of TMB, which is widely used colorimetric peroxidase substrate, in the presence of H_2O_2. **Figure 3** reveals that all the MOFs-TMB-H_2O_2 systems developed a deep blue color indicative of their peroxidase-like activity while there was no significant color change observed in the absence of the catalyst. Two representative absorption peaks centered at 370 and 650 nm were observed, which originated from the oxidation of TMB. It has already been proposed that Fe-MOFs with Fe(III) as active metal center can oxidize TMB molecules

through the production of OH radicals, which derive from the catalytic decomposition of H_2O_2, simultaneously yielding a blue colored, oxidized TMB (oxTMB) (Dong et al. 2015; Liu et al. 2013; Kim et al. 2014c). We further found that the peroxidase-like activity of MIL-100(Fe) was significantly improved after the functionalization with amines, as shown in Figure 3. Among the amine modified MIL-100(Fe), TMBDA-MIL-100(Fe) yielded the highest absorption intensity, approximately 2-fold higher than that of MIL-100(Fe) without any amine modification.

The increased amount of negative charges on the particles of amine-functionalized MOFs could help to improve their affinity towards positively charged TMB molecules through an electrostatic attraction. This type of phenomenon has been previously reported for the TMB substrate using different negatively charged materials (Ju et al. 2016; Ma et al. 2015; Yu et al. 2009). Among the various amine-grafted MOFs, TMBDA-MIL-100(Fe) was demonstrated to exhibit the highest peroxidase-like activity. It was observed that, in spite of having the largest negative potential (-30.3 eV) among the tested MOFs, DMPDA-MIL-100(Fe) displayed a lower peroxidase-like activity than TMBDA-MIL-100(Fe), suggesting that a high negative potential could not be the sole reason for the improved catalytic activity. The grafted diamines further differ in molecular size (**Table S2**), and consequently in their hydrophobic nature due to the extension of the carbon chain between the two nitrogen atoms and the replacement of the hydrogens on the nitrogen atoms by methyl groups. The peroxidase-like activity of amine-grafted MIL-100(Fe) increased as the molecular size and hydrophobic

nature of the grafted amines increased (ED < DMPDA < TMBDA). This confirmed that the difference in size and hydrophobicity among the grafted diamines could also contribute to the catalytic activity of MOFs along with the electrostatic interactions, as demonstrated by the previous report that a slight change in the hydrophobicity of the environment around the reaction center in MOF structures could significantly modify the substrate selectivity in aldol-type condensation reactions (Abedi et al. 2016). In an another example, Kim et al. successfully grafted diethylenetriamine (DETA) on CUS of MIL-101(Cr) and confirmed that hydrophilic nature of the pristine MIL-101(Cr) turns hydrophobic after DETA grafting which significantly affect the heat of CO_2 adsorption and CO_2 adsorption capacity in its porous structure (Kim et al. 2012).

To gain a further insight into this phenomenon, we grafted 1,8-octanediamine (ODA) onto the CUS of MIL-100(Fe) (see **Figure S2** in the supporting information for further details). The ODA-grafted MIL-100(Fe) was employed in peroxidase-mediated colorimetric reactions and found to be inferior compared to all other amine modified MIL-100(Fe) (**Figure S3**). Therefore, the presence of a longer carbon chain in the amine can partially shield the active iron domain present on the MOF surface, which possesses catalytic activity to oxidize the TMB molecules, resulting in a decreased activity. This result is in agreement with the findings of Yu *et al.*, who studied the impact of coating on the peroxidase activity of Fe_3O_4 nanoparticles, and discovered that a thicker coating could shield the active iron domains on the surface of the particles hampering their peroxidase-like activity, although the coating

imparted negative charges on the iron oxide surface that generally enhance the catalytic activity (Yu et al. 2009). Therefore, the synergistic effect of the increased negative surface charge and controlled molecular size of the grafted diamines on MIL-100(Fe) helped to attract the substrate molecules near the active centers via electrostatic and hydrophobic interactions which lead to a significantly improved peroxidase-like activity. Moreover, the peroxidase-like activity of TMBDA-MIL-100(Fe) was also confirmed by the catalytic oxidation of a highly sensitive AUR substrate in the presence of H_2O_2, which produced an intense fluorescence signal and were used in further studies (**Figure S4**).

3.3. Investigation for peroxidase-like activity of TMBDA-MIL-100(Fe) on the oxidation of AUR

Similar to HRP, the peroxidase-like activity of TMBDA-MIL-100(Fe) varied significantly depending on pH, temperature, and concentrations of buffer and catalyst itself (**Figure S5**). The peroxidase-like activity of TMBDA-MIL-100(Fe) was measured by varying the temperature from 20 to 80 °C (**Figure S5a**) and the pH from 2 to 12 (**Figure S5b**). Under the typical conditions to measure the peroxidase-like activity with AUR substrate, TMBDA-MIL-100(Fe) showed the highest catalytic activity at around neutral pH and retained a considerable amount of activity (over 80% of the maximal activity) over a broad range of temperatures (20-60 °C). We also studied the effects of the MOF and buffer concentrations

within a range of 0.05-0.2 mg/mL and 1-25 mM, respectively (**Figure S5c and S5d**). The maximal catalytic activity was observed with 0.2 mg/mL MOF and 5 mM buffer concentrations. Thus, the optimal conditions were chosen as pH 7, 37 °C, 0.2 mg/mL MOF, and 5 mM Tris acetate buffer.

Since the peroxidase-like activity of TMBDA-MIL-100(Fe) is promoted by H_2O_2, this system was employed to detect the H_2O_2 dissolved in sample solution. The fluorescence intensity upon oxidation of AUR sharply increased with increasing H_2O_2 concentrations from 1 to 500 µM **(Figure S5e)**. As shown in the inset of Figure S5e, a linear relationship (R^2 = 0.9904) between fluorescence intensity and H_2O_2 concentration in a range of 1–30 µM with a low detection limit of 0.329 µM was obtained, which implies that the TMBDA-MIL-100(Fe) catalytic system could be used in analytical systems for the detection of H_2O_2. This level of sensitivity is sufficient to enable coupling of the MOF system with any oxidase to create versatile biosensor (Kim et al. 2011b; Shin et al. 2017). Moreover, TMBDA-MIL-100(Fe) was shown to have good recyclability up to five times with a negligible loss of catalytic activity (**Figure S6a**). This minor loss in activity was presumably due to the incomplete recovery of the MOF nanoparticles from the reaction solution by centrifugation after each cycle. The structure of this MOF remained unchanged after five recycle tests, as confirmed by SEM analysis (**Figure S6b**).

3.4. Steady-state kinetic assay of amine-grafted MIL-100(Fe)

The peroxidase-like activity of TMBDA-MIL-100(Fe) was further investigated through a

steady-state kinetic assay. Within the suitable ranges of H_2O_2 and TMB concentrations, typical Michaelis–Menten curves were obtained for TMBDA-MIL-100(Fe) (**Figure S7**). The kinetic parameters such as the maximum initial velocity (Vmax) and Michaelis–Menten constant (K_m) were determined using Lineweaver–Burk plots (**Table 1**).

The apparent K_m of TMBDA-MIL-100(Fe) with TMB as substrate was at least five times lower than that of HRP and the original MIL-100(Fe), which suggests that TMBDA-MIL-100(Fe) has a higher affinity toward TMB than HRP and MIL-100(Fe). The K_m value of TMBDA-MIL-100(Fe) with H_2O_2 as substrate was at least two times lower than that of HRP and MIL-100(Fe), which is consistent with the values of other peroxidase-mimetic Fe-MOFs (Table 1), suggesting that TMBDA-MIL-100(Fe) has a higher affinity to H_2O_2 than HRP and MIL-100(Fe). This improved catalytic performance of TMBDA-MIL-100(Fe) could most likely be attributed to the occurrence of interface amine moieties on the surface of the MOF, which helped to attract the substrate molecules near the active centers via electrostatic and hydrophobic interactions. This phenomenon is similar to the mechanism of natural enzymes, which possess extraordinary catalytic activities due to their ability to bring the substrates into close proximity with their active centers (Garcia-Viloca et al. 2004; Song et al. 2010a; Tao et al. 2013).

3.5. Detection of choline by employing TMBDA-MIL-100(Fe)

Choline is related to the B vitamins and is involved in brain development, muscle movement, and body metabolism (Biswas and Giri 2015). Moreover, it is the precursor of acetylcholine,

which is an important neurotransmitter in the peripheral nervous system (Wei et al. 2014). In spite of being produced in the human body, its dietary supplementation is required in order to maintain a proper functionality (Blusztajn 1998). Accordingly, choline is widely added in food such as milk and dietary supplements (Chen et al. 2011; Phillips 2012). However, the inadequate level of choline in the body may cause several diseases such as neural tube defects, Alzheimer's and fatty liver disease (Biswas and Giri 2015; Phillips 2012). Therefore, an effective detection method is of utmost importance to monitor an adequate level of choline in the body.

Hence, based on the excellent peroxidase-like activity of TMBDA-MIL-100(Fe) for H_2O_2 detection, we developed a simple fluorescent method for the detection of choline. As shown in equations 1 and 2, choline can be hydrolyzed by choline oxidase to generate H_2O_2 that can be utilized in the catalytic oxidation of AUR in the presence of TMBDA-MIL-100(Fe) to produce oxidized AUR. OxAUR generates fluorescence upon excitation at 588 nm, which can be used to quantify choline.

$$Choline + O_2 + H_2O \xrightarrow{\text{Choline oxidase}} betaine + H_2O_2 \quad \text{..... (1)}$$

$$H_2O_2 + AUR \xrightarrow{\text{TMBDA-MIL-100(Fe)}} H_2O + OxAUR \quad \text{.....(2)}$$

To determine the optimum conditions, the fluorescence intensity resulting from the oxidation of AUR was measured by varying the pH, temperature, and concentration of ChOx and TMBDA-MIL-100(Fe) (**Figure 4 a-d**). The obtained optimum conditions were 0.6 U/mL of ChOx, 0.2 mg/mL of TMBDA-MIL-100(Fe), pH 7, and 37 °C. Under these conditions, target

choline was successfully detected by the generation of fluorescence intensity corresponding to oxidized AUR (**Figure S8**). On the other hand, no meaningful signal was observed in the negative control samples, where other molecules (glucose, lactose, glycine, aspartic acid, and glutathione) similar to the target choline were used even at 10-fold higher concentrations. This result clearly demonstrates that the present assay is highly selective toward target choline in the presence of other interfering molecules, presumably due to the high specificity of ChOx. A good linear correlation (R^2 = 0.9907) was also observed between the fluorescent intensity and the concentration of choline in a range of 0.5–10 μM (**Figure 4e**). The limit of detection (LOD) (0.027 μM) for the proposed biosensor is among the best results of those found in recent reports describing choline detection (**Table S3**), indicating the importance of the significantly enhanced peroxidase-like activity of amine-grafted MIL-100(Fe) on the performance of choline assay.

In order to explore the practical capability of the proposed method, we detected choline in milk through a standard addition method. As a result shown in **Table S4**, the mean recovery for choline was around 100%, clearly demonstrating that our proposed choline sensing method could be employed to detect choline in real samples.

3.6. Detection of acetylcholine (ACh) by employing TMBDA-MIL-100(Fe)

Acetylcholine plays a vital role in both peripheral and central nervous systems. It is involved in brain functions such as alertness, learning, and memory. Patients with neural disorders such as Alzheimer's disease (AD), Parkinson disease, schizophrenia, and progressive

dementia were found to have decreased ACh levels (Ehrenstein et al. 1997; He et al. 2014; Ren et al. 2015). In order to treat these diseases, the quantification of ACh in biological samples such as blood and neuronal cells is of utmost importance.

$$Acetylcholine \xrightarrow{\text{Acetylcholinesterase}} Choline + acetic\ acid \quad \text{.....(3)}$$

The hydrolysis of ACh can be catalyzed by acetylcholine esterase to produce choline (Eq. (3)), which subsequently undergoes a catalytic process promoted by ChOx to give H_2O_2 (Eq. (1)); MOFs can utilize this H_2O_2 for the oxidation of AUR developing a fluorescence intensity (Eq. (2)). To implement this strategy, first the time-dependent kinetics were determined with and without acetylcholine (**Figure 5a**), and thereafter the optimized conditions such as temperature and pH were determined to be 37 °C and 7 (**Figure 5 b** and **c**), respectively. Through the typical reaction, only the target ACh induced a dramatic increase of the respective fluorescence intensity (**Figure S9**), indicating that this fluorescent assay is highly selective toward the target ACh in the presence of typical interfering molecules even at 10-fold concentrations. This high selectivity is mainly due to the high specificity of AChE and ChOx toward ACh and choline, respectively. Consequently, as shown in **Figure 5d**, a linear relationship (R^2 = 0.9902) between fluorescence intensity and acetylcholine concentration in a range of 0.1–10 µM with a detection limit of 0.036 µM was obtained. This LOD was among the best results when compared with recently reported biosensors used for the detection of acetylcholine (**Table S5**), confirming the high sensitivity of our acetylcholine assay arisen from the excellent peroxidase-like activity of amine-grafted MIL-100(Fe).

Inspired by the high sensitivity of our sensing system for the detection of acetylcholine, we endeavored to detect acetylcholine in serum (10%) through a standard addition method. The obtained results (**Table S6**) are in good agreement with the added acetylcholine, showing around 97-103% recovery for acetylcholine, and suggesting that the developed method is applicable for the detection of acetylcholine in real serum samples.

4. Conclusions

In this study, we successfully synthesized various diamine-grafted MIL-100(Fe) and for the first time systematically investigated their peroxidase-like activity. The characterization data of the amine-grafted MIL-100(Fe) were well correlated with their peroxidase-mimicking activity and it was suggested that the improved catalytic activity was due to the enhanced negative potential of the amine-grafted MIL-100(Fe) and controlled size of the grafted diamine, which helped to bring the substrate in close proximity with the active Fe(III) centers present on the MOF surface. However, the detection mechanism underlying these effects remains to be determined. We further utilized the highly enhanced peroxidase activity of the amine-grafted MIL-100(Fe) to develop a simple fluorescent assay to detect choline and acetylcholine with significantly low detection limits (0.027 and 0.036 μM respectively). The present work encouraging the further investigations in post-synthetic functionalization of

MOFs to design new functional nanomaterials as enzymatic mimetics capable of detecting biomolecules.

Acknowledgments

This work was supported by the R&D Program of the Institutional Research Program of KRICT (SI1701-02), and partly by the Defense Industry Technology Center (DITC) of Korea (contract grant number UC15000ID). JSC is kindly grateful to the National Research Council of Science and Technology (NST) for financial support (KN16-15). This work was also supported by the Mid-career Researcher Support Program through the National Research Foundation (NRF) funded by the Ministry of Science, ICT & Future planning (MSIP) of Korea (No. 2015R1A2A1A01005393).

References

Abedi, S., Tehrani, A.A., Ghasempour, H., Morsali, A., 2016. New J Chem 40(8), 6970-6976.

Ai, L.H., Li, L.L., Zhang, C.H., Fu, J., Jiang, J., 2013. Chem-Eur J 19(45), 15105-15108.

Asati, A., Santra, S., Kaittanis, C., Nath, S., Perez, J.M., 2009. Angew Chem Int Ed 48(13), 2308-2312.

Banerjee, M., Das, S., Yoon, M., Choi, H.J., Hyun, M.H., Park, S.M., Seo, G., Kim, K., 2009. J Am Chem Soc 131(22), 7524-7525.

Batule, B.S., Park, K.S., Kim, M.I., Park, H.G., 2015. Int J Nanomedicine 10, 137-142.

Biswas, S., Giri, S., 2015. Prague Med Rep 116(1), 5-15.

Blusztajn, J.K., 1998. Science 281(5378), 794-795.

Cabello, C.P., Berlier, G., Magnacca, G., Rumori, P., Palomino, G.T., 2015. Cryst Eng Comm 17(2), 430-437.

Chen, Z., Ren, X., Meng, X., Chen, D., Yan, C., Ren, J., Yuan, Y., Tang, F., 2011. Biosens Bioelectron 28(1), 50-55.

Desai, A.V., Samanta, P., Manna, B., Ghosh, S.K., 2015. Chem Commun 51(28), 6111-6114.

Dinca, M., Han, W.S., Liu, Y., Dailly, A., Brown, C.M., Long, J.R., 2007. Angew Chem Int Ed 46(9), 1419-1422.

Dong, W., Liu, X., Shi, W., Huang, Y., 2015. Rsc Adv 5(23), 17451-17457.

Ehrenstein, G., Galdzicki, Z., Lange, G.D., 1997. Biophys J 73(3), 1276-1280.

Feng, D.W., Gu, Z.Y., Li, J.R., Jiang, H.L., Wei, Z.W., Zhou, H.C., 2012. Angew Chem Int Ed 51(41), 10307-10310.

Filizola, M., Loew, G.H., 2000. J Am Chem Soc 122(1), 18-25.

Gao, L.Z., Zhuang, J., Nie, L., Zhang, J.B., Zhang, Y., Gu, N., Wang, T.H., Feng, J., Yang, D.L., Perrett, S., Yan, X., 2007. Nat Nanotechnol 2(9), 577-583.

Garcia-Viloca, M., Gao, J., Karplus, M., Truhlar, D.G., 2004. Science 303(5655), 186-195.

He, S.B., Wu, G.W., Deng, H.H., Liu, A.L., Lin, X.H., Xia, X.H., Chen, W., 2014. Biosens Bioelectron 62, 331-336.

Horcajada P., Surble S., Serre C., Hong D.Y.,. Seo Y.K, Chang J.S., Greneche J.M., Margiolaki I., Ferey G., 2007. Chem. Commun 2820–2822.

Hwang, Y.K., Hong, D.Y., Chang, J.S., Jhung, S.H., Seo, Y.K., Kim, J., Vimont, A., Daturi, M., Serre, C., Ferey, G., 2008. Angew Chem Int Ed 47(22), 4144-4148.

Ju, P., Xiang, Y., Xiang, Z., Wang, M., Zhao, Y., Zhang, D., Yu, J., Han, X., 2016. Rsc Adv 6(21), 17483-17493.

Kasinathan, P., Seo, Y.-K., Shim, K.-E., Hwang, Y.K., Lee, U.-H., Hwang, D.W., Hong, D.-Y., Halligudi, S.B., Chang, J.-S., 2011. Bull Korean Chem Soc 32(6), 2073-2075.

Kim, M.I., Ye, Y., Won, B.Y., Shin, S., Lee, J., Park, H.G., 2011a. Adv Funct Mater 21(15), 2868-2875.

Kim, M.I., Shim, J., Li, T., Lee, J., Park, H.G., 2011b. Chem Eur J 17(38), 10700-10707.

Kim, S.-N., Yang, S.-T., Kim, J. Park J.-E., Ahn, W.-S.,2012. CrystEngComm 14, 4142-4147.

Kim, M.I., Ye, Y., Woo, M.A., Lee, J., Park, H.G., 2014a. Adv Healthcare Mater 3(1), 36-41.

Kim, M.I., Kim, M.S., Woo, M.A., Ye, Y., Kang, K.S., Lee, J., Park, H.G., 2014b. Nanoscale 6(3), 1529-1536.

Kim, M.I., Park, K.S., Park, H.G., 2014c. Chem Commun 50(67), 9577-9580.

Kumar, P., Deep, A., Kim, K.-H., 2015. Trends in Anal Chem 73, 39-53.

Larsen, R.W., Wojtas, L., Perman, J., Musselman, R.L., Zaworotko, M.J., Vetromile, C.M., 2011. J Am Chem Soc 133(27), 10356-10359.

Lee, J., Farha, O.K., Roberts, J., Scheidt, K.A., Nguyen, S.T., Hupp, J.T., 2009. Chem Soc Rev 38(5), 1450-1459.

Lee, Y.C., Kim, M.I., Woo, M.A., Park, H.G., Han, J.I., 2013. Biosens Bioelectron 42, 373-378.

Li, J.R., Sculley, J., Zhou, H.C., 2012. Chem Rev 112(2), 869-932.

Liu, Y.L., Zhao, X.J., Yang, X.X., Li, Y.F., 2013. Analyst 138(16), 4526-4531.

Llewellyn, P.L., Bourrelly, S., Serre, C., Vimont, A., Daturi, M., Hamon, L., De Weireld, G., Chang, J.S., Hong, D.Y., Kyu Hwang, Y., Hwa Jhung, S., Ferey, G., 2008. Langmuir 24(14), 7245-7250.

Ma, Z., Qiu, Y., Yang, H., Huang, Y., Liu, J., Lu, Y., Zhang, C., Hu, P., 2015. ACS Appl Mater Interfaces 7(39), 22036-22045.

Meilikhov, M., Furukawa, S., Hirai, K., Fischer, R.A., Kitagawa, S., 2013. Angew Chem Int Ed 52(1), 341-345.

Mu, J.S., Wang, Y., Zhao, M., Zhang, L., 2012. Chem Commun 48(19), 2540-2542.

Murray, L.J., Dinca, M., Long, J.R., 2009. Chem Soc Rev 38(5), 1294-1314.

Nagarkar, S.S., Joarder, B., Chaudhari, A.K., Mukherjee, S., Ghosh, S.K., 2013. Angew Chem Int Ed 52(10), 2881-2885.

Park, K.S., Batule, B.S., Chung, M., Kang, K.S., Park, T.J., Kim, M.I., Park, H.G., 2017. J Mater Chem B 5(12), 2231-2234.

Phillips, M.M., 2012. Anal Bioanal Chem 403(8), 2103-2112.

Qin F. X., Jia S. Y., Wang F. F., Wu S. H., Song J., Liu Y., 2013. Catal Sci Technol 3, 2761.

Ren, X., Wei, J., Ren, J., Qiang, L., Tang, F., Meng, X., 2015. Colloids Surf B Biointerfaces 125, 90-95.

Rodríguez-López, J.N., Lowe, D.J., Hernández-Ruiz, J., Hiner, A.N., García-Cánovas, F., Thorneley, R.N., 2001. J Am Chem Soc 123(48), 11838-11847

Seo, Y.-K., Yoon, J.W., Lee, J.S., Lee, U.-H., Hwang, Y.K., Jun, C.-H., Horcajada, P., Serre, C., Chang, J.-S., 2012. Micropor Mesopor Mat 157, 137-145.

Shi, W., Wang, Q., Long, Y., Cheng, Z., Chen, S., Zheng, H., Huang, Y., 2011. Chem Commun 47(23), 6695-6697.

Shin, H.Y., Kim, B.G., Cho, S., Lee, J., Na, H.B., Kim, M.I., 2017. Microchim Acta 184(7), 2115-2122.

Song, Y., Qu, K., Xu, C., Ren, J., Qu, X., 2010a. Chem Commun 46(35), 6572-6574.

Song, Y., Qu, K., Zhao, C., Ren, J., Qu, X., 2010b. Adv Mater 22(19), 2206-2210.

Song, Y.J., Wang, X.H., Zhao, C., Qu, K.G., Ren, J.S., Qu, X.G., 2010c. Chem Eur J 16(12), 3617-3621.

Tanabe, K.K., Cohen, S.M., 2011. Chem Soc Rev 40(2), 498-519.

Tao, Y., Lin, Y., Huang, Z., Ren, J., Qu, X., 2013. Adv Mater 25(18), 2594-2599.

Valekar, A.H., Cho, K.-H., Chitale, S.K., Hong, D.-Y., Cha, G.-Y., Lee, U.-H., Hwang, D.W., Serre, C., Chang, J.-S., Hwang, Y.K., 2016. Green Chem 18(16), 4542-4552.

Veitch, N.C., 2004. Phytochemistry 65(3), 249-259

Wang, Z., Cohen, S.M., 2009. J Am Chem Soc 131(46), 16675-16677.

Wei, H., Wang, E., 2013. Chem Soc Rev 42(14), 6060-6093.

Wei, J., Ren, J., Liu, J., Meng, X., Ren, X., Chen, Z., Tang, F., 2014. Biosens Bioelectron 52, 304-309.

Wuttke, S., Bazin, P., Vimont, A., Serre, C., Seo, Y.K., Hwang, Y.K., Chang, J.S., Ferey, G., Daturi, M., 2012. Chemistry 18(38), 11959-11967.

Yu, F., Huang, Y., Cole, A.J., Yang, V.C., 2009. Biomaterials 30(27), 4716-4722.

Zhang, J.W., Zhang, H.T., Du, Z.Y., Wang, X.Q., Yua, S.H., Jiang, H.L., 2014. Chem Commun 50(9), 1092-1094.

Zimpel, A., Prei, T., Röder, R., Engelke, H., Ingrisch, M., Peller, M., Rädler, J.O., Wagner, E., Bein, T., Lächelt, U., 2016. Chem Mater 28(10), 3318-3326.

Figures and Table

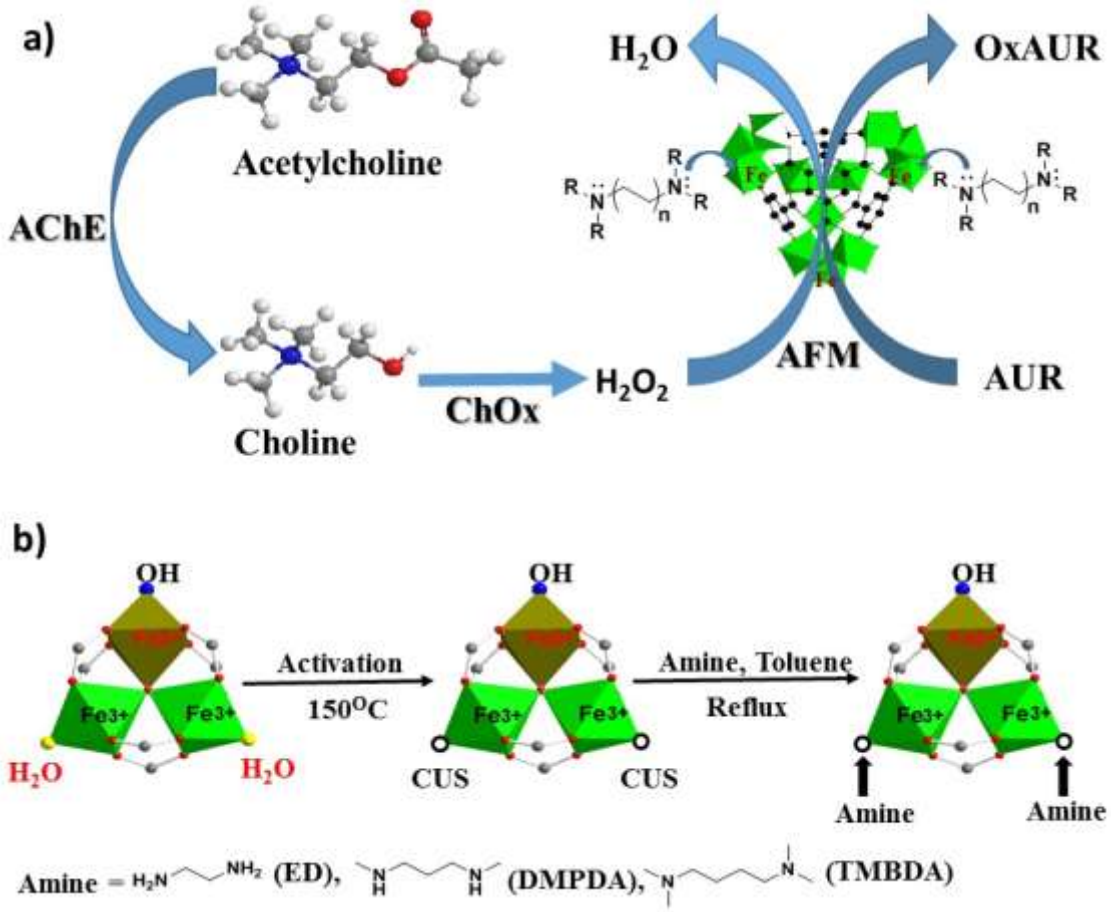

Figure 1. a) Schematic representation of the proposed fluorescence method for the detection of acetylcholine and choline, and b) Grafting of diamines on coordinatively unsaturated sites of MIL-100(Fe).

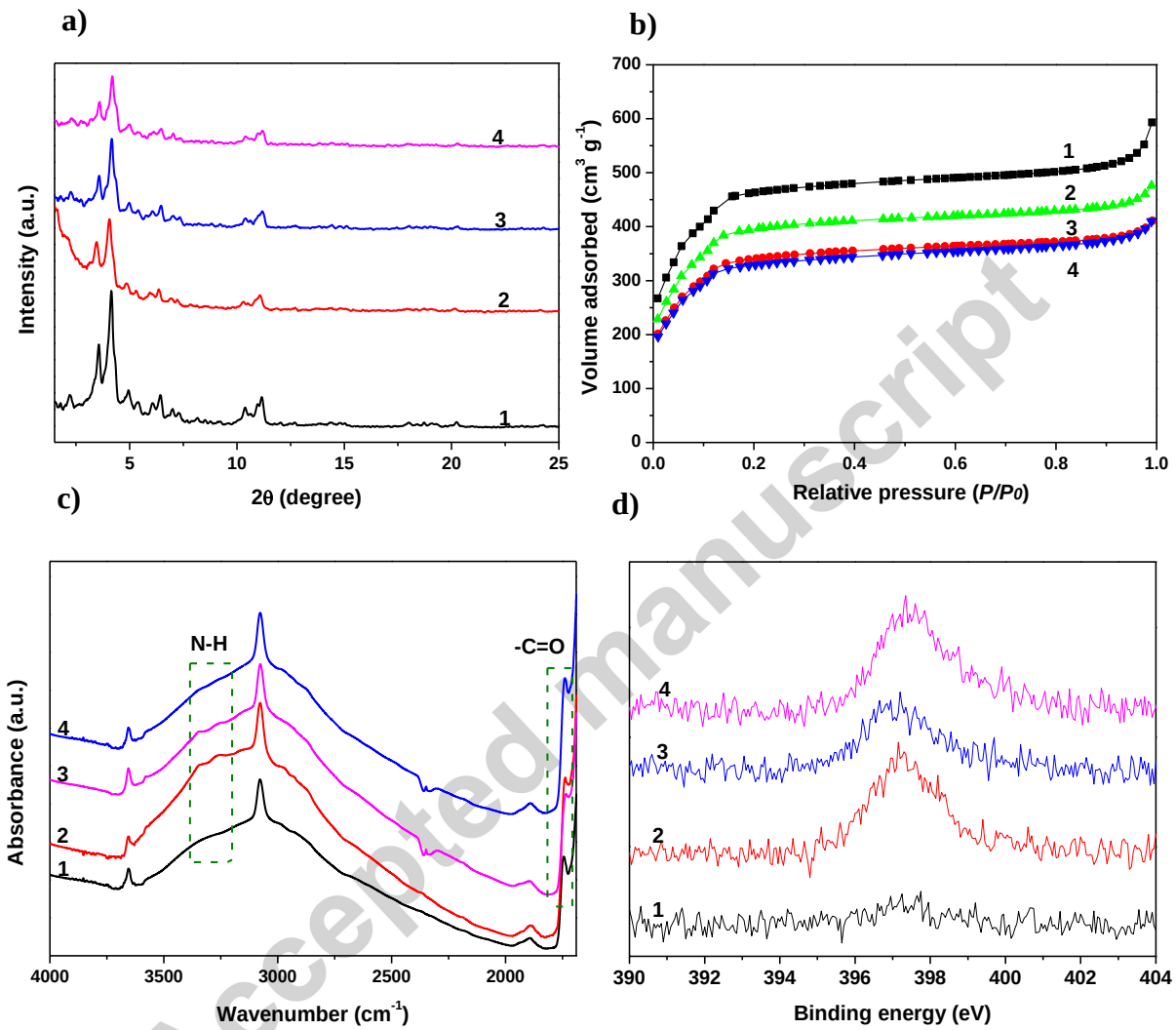

Figure 2. a) XRPD patterns, b) N_2 physisorption at 77 K, and c) FT-IR spectra at 423 K and d) XPS analysis (N1s) of pristine and amine grafted MIL-100(Fe). **1**. Pristine MIL-100(Fe), **2**. ED-MIL-100(Fe), **3**. DMPDA-MIL-100(Fe), and **4**.TMBDA-MIL-100(Fe).

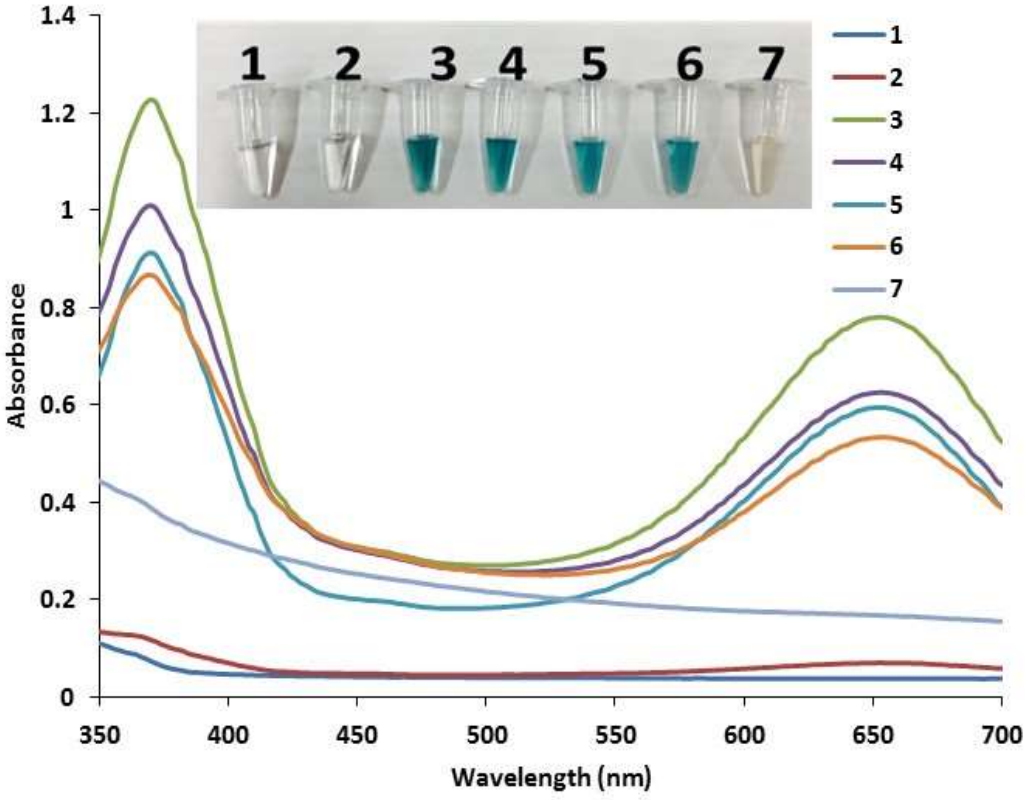

Figure 3. Comparison of the peroxidase-mimic activity of pristine and various amines grafted MIL-100(Fe) to promote the oxidation of TMB substrate. 1. TMB, 2. TMB + H_2O_2, 3. TMB + H_2O_2 + TMBDA-MIL-100(Fe), 4. TMB + H_2O_2 + DMPDA-MIL-100(Fe), 5. TMB + H_2O_2 + ED-MIL-100(Fe), 6. TMB + H_2O_2 + MIL-100 (Fe), 7. TMB + TMBDA-MIL-100(Fe). Detection conditions: 5 mM (pH 4), Tris acetate buffer, 1 mM H_2O_2, 0.2 mg/mL MOF, 1 mM TMB, 40 °C for 20 min; Absorbance: 350-700 (370 nm, 650 nm).

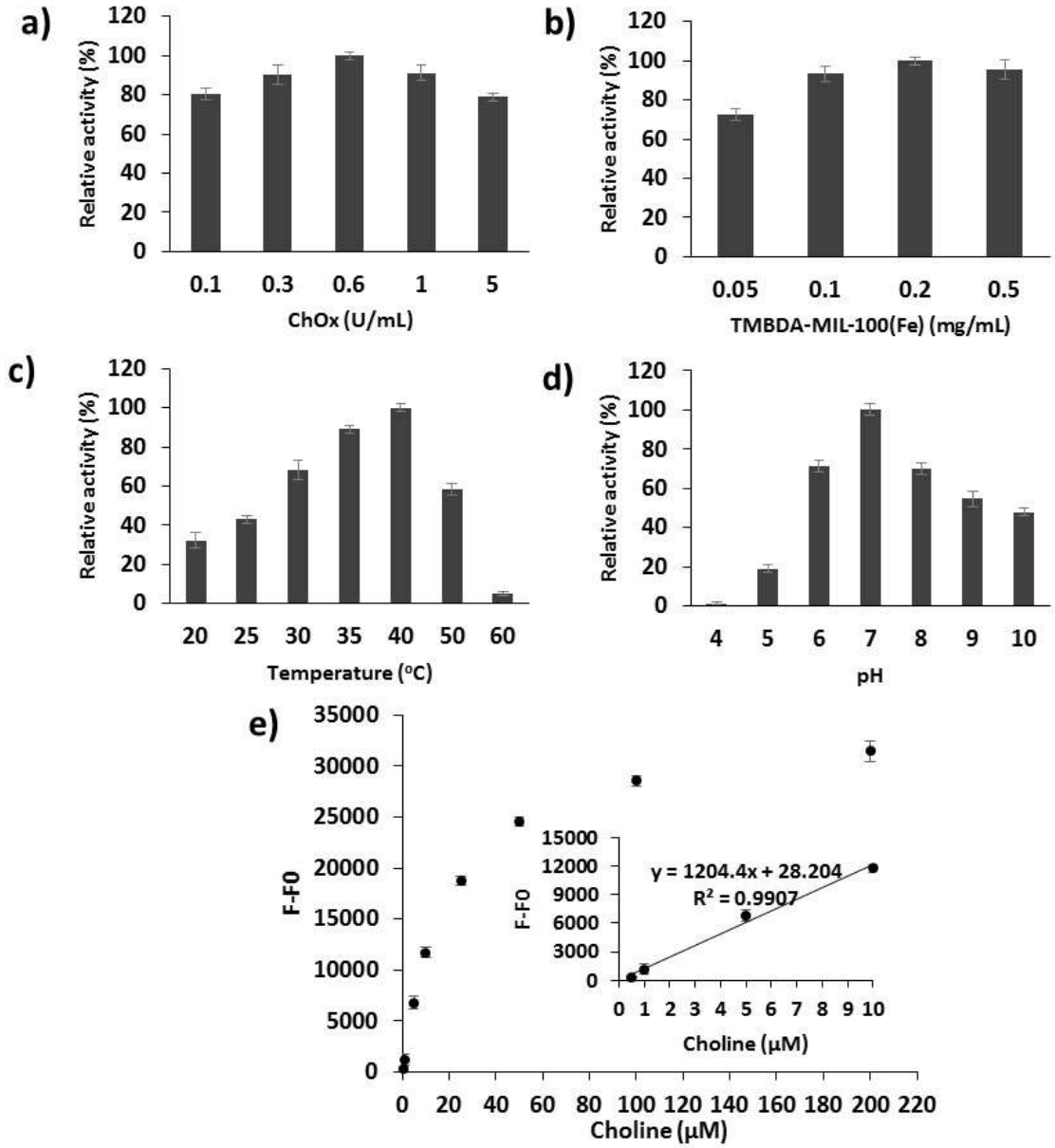

Figure 4. Effect of concentration of a) ChOx (U/mL), b) of TMBDA-MIL-100(Fe) (mg/mL). c) Effect of temperature, and (d) pH on catalytic activity of TMBDA-MIL-100(Fe). e) Choline concentration-dependent change of the fluorescence intensity; the inset shows the linear range between the fluorescence intensity and choline concentration (0.5–10 μM).The fluorescence intensity is defined as $F\text{-}F_0$, where F_0 and F are the fluorescence intensities measured at excitation 540 nm and emission at 588 nm in the absence and presence of choline, respectively. Relative activity (%) was determined by using the ratio of the colorimetric activity to the maximal activity at each graph.

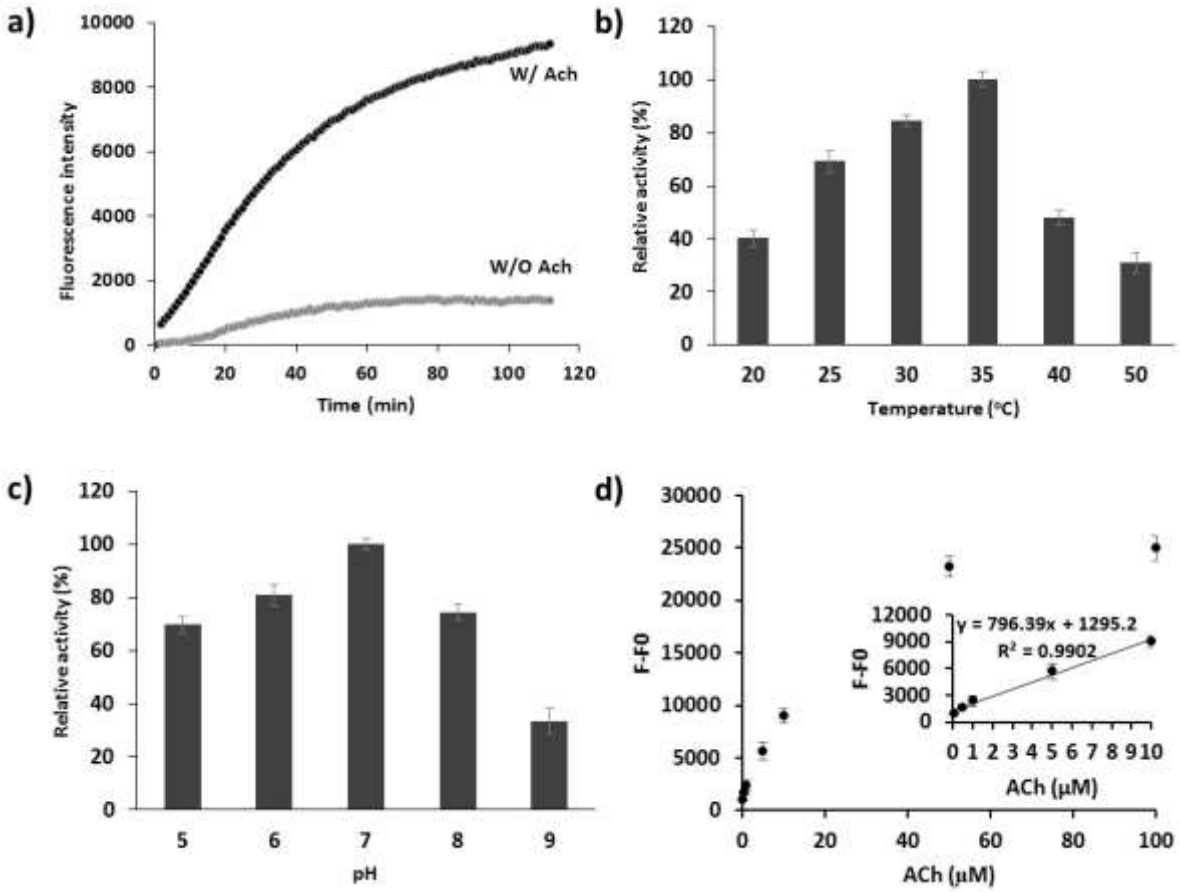

Figure 5. (a) Time-dependent fluorescence intensities (λmax = 588 nm) of reaction mixtures containing W/ and W/O Ach, (b) Effect of temperature, (c) Effect of pH on catalytic activity of TMBDA-MIL-100(Fe), and (d) ACh concentration-dependent change of the fluorescence intensity; the inset shows the linear range between the fluorescence intensity and ACh concentration (0.1–10 μM). The fluorescence intensity is defined as $F\text{-}F_0$, where F_0 and F are the fluorescence intensities measured at excitation 540 nm and emission at 588 nm in the absence and presence of acetylcholine, respectively. Relative activity (%) was determined by using the ratio of the colorimetric activity to the maximal activity at each graph.

Table 1. Comparison of the apparent Michaelis–Menten constant (Km) and maximum reaction rate (Vmax) of TMBDA-MIL-100(Fe) and other peroxidase mimics.

Catalyst	*K*m/mM		Vmax/10^{-8} M S^{-1}		Reference
	H_2O_2	TMB	H_2O_2	TMB	
HRP	0.055	0.317	2.43	3.30	(Liu et al. 2013)
MIL-100(Fe)	0.064	0.424	1.4	2.1	This work
TMBDA-MIL-100(Fe)	0.028	0.062	23.3	45	This work
MIL-53(Fe) by CE	0.04	1.08	1.86	8.78	(Ai et al. 2013)
MIL-53(Fe) by MW	0.03	0.28	0.96	4.48	(Dong et al. 2015)
Fe-MIL-88-NH_2	0.206	0.284	7.04	10.47	(Liu et al. 2013)

Highlights

- Various aliphatic diamines were grafted on coordinatively unsaturated metals sites of MIL-100(Fe) and subjected for peroxidase-like activity.
- Enhanced peroxidase-like activity of amine functionalized MIL-100(Fe) (AFM) originated from synergetic effect of enhanced negative potential and precisely controlled molecular size of grafted diamines.
- Based on the excellent peroxidase-like activity of AFM, a simple and sensitive fluorescent detection of choline and acetylcholine was successfully performed.
- Effectively determined choline and acetylcholine levels in real samples of milk and serum, respectively.